Progress In Electromagnetics Research C, Vol. 127, 113–125, 2022

4-Port MIMO Antenna for Sub-1 GHz, IoT, and Sub-6 GHz 5G New Radio Applications

Bisma Bukhari* **and Ghulam M. Rather**

Abstract—A 4-port planar multiple-input multiple-output (MIMO) antenna system design is proposed. The antenna elements are modified meandered wideband antennas which cover frequencies from 674 MHz to 1 GHz, 1.9 GHz to 2.1 GHz, 3.175 GHz to 3.476 GHz, 4.529 GHz to 4.761 GHz, and 5.254 to 5.513 GHz for long term evolution (LTE), Internet of Things (IoT), and sub-6 GHz applications and thus can be used for robotic navigation, logistics, healthcare, tracking, transportation, etc. Due to very small envelope correlation coefficient (ECC) between the ports (< 0.5), the MIMO configuration can be efficiently implemented which helps in increasing the data rates. It is very compact in size and thus can be used for portable handheld devices. Since there is the problem of current localization due to common ground, the future work aims at minimizing coupling and improving the impedance matching using novel decoupling networks. These MIMO antennas are connected to a common slotted ground plane. Antenna simulation has been done using Computer Simulation Technology (CST) Microwave Studio Suite simulator. A low cost FR-4 substrate with dimensions 65 mm × 90 mm × 1.6 mm has been used for antenna fabrication, and experimental results are obtained using an anechoic chamber and a vector network analyser. ECC and realized gain of the antenna are also obtained experimentally and are almost similar to the simulated results.

1. INTRODUCTION

Applications like Long term evolution (LTE), Internet of Things (IoT), Radio Frequency Identification (RFID), Cognitive Radio (CR), and 5G New Radio demand high data rates, link reliability, compact size, and good quality of service. Also, due to the integration of multiple wireless standards on the same device, antennas having multi-functionalities are highly desirable for latest wireless applications [1–3]. The implementation of MIMO provides a secure and efficient wireless connection between the users in addition to good quality of service to various communication standards like CR, LTE, 5G, etc. [4–10]. CR performs dynamic spectrum management and thus increases the spectral efficiency. Because of the scaling down of wireless circuits, the need of next generation technologies like LTE with higher data rates is growing day by day [11–18]. So, designing a compact MIMO antenna to cover sub-1 GHz bands like LTE 700 without increasing the antenna size and decreasing its performance is one of the design challenges. IoT is an automated platform for next generation applications like robotic navigation, smart sensors, logistics, healthcare tracking transportation, etc. [19–21]. It enables widespread connectivity of small objects to the Internet. Many antenna design issues must be overcome in order to provide these services, including the need for multi-standard antennas with low profile structures, more compact sizes for small IoT devices, and lower costs. IoT employs current RFID techniques. Depending upon the application, the RFID techniques use 840 MHz to 960 MHz, 2.4 GHz to 2.48 GHz, and 5.72 GHz to 5.87 GHz frequency bands [22]. Previously, there were separate antennas for different applications which made the antenna systems bulky. Due to the miniaturization of devices, various wireless standards need

Received 7 September 2022, Accepted 22 November 2022, Scheduled 30 November 2022
* Corresponding author: Bisma Bukhari (bismabukhari11@gmail.com).
The authors are with the Department of Electronics and Communication Engineering, NIT Srinagar, J&K, 190006, India.

to be integrated on the same compact antenna while maintaining optimum antenna performance [3, 7]. Since the antenna has to cover multiple frequency bands, another challenge is to design an antenna for both the low and high ends of spectrum [10, 13, 21–22]. Other challenges include less MIMO antenna coupling and ECC. LTE antennas with MIMO implementation are presented in [11–13] which cover 4G LTE, GSM 900, WLAN bands, etc. For impedance matching, defected ground surface (DGS) and via holes are used, but they affect the antenna performance. Additional extensions are also added on the ground which increases complexity and leads to parasitic resonances. Antennas for sub-6 GHz bands and IoT are presented in [14–18]. Though these antennas cover many important wireless bands, they do not cover sub-1 GHz frequency bands. Also, only a few frequency bands [15] are covered. Other drawbacks are that most of them are large in size [16] or are implemented in single input single output (SISO) configuration [17].

The SISO implementation of CR antennas is presented in [23–29]. The antenna elements have poor isolation, and the tuning circuits used in them make the system bulky. Also, they have a very narrow sensing range and fail to cover sub-6 GHz frequency bands like LTE 700. So, MIMO implementation is extremely useful for increasing the data rates and channel capacity. MIMO antennas for some of the applications are presented in [34–36]. Though multiple bands are covered by these antennas, they are unable to cover sub-1 GHz bands and other important sub-6 GHz bands. Most of the works investigated only a few performance parameters like radiation characteristics but not paying much attention towards important parameters like directivity, gain, envelope correlation coefficient (ECC), etc.

Keeping in view the above drawbacks and for integrating RFID, IoT, LTE, and various other important 5G NR sub-6 GHz standards on the same compact device, a planar multiband and multistandard 4-port MIMO antenna is proposed. Antenna 1 to antenna 4 are placed at four corners on the top of an FR-4 substrate with a slotted ground at the bottom. The MIMO antenna operates over bands like 674 MHz to 1 GHz, 1.9 GHz to 2.1 GHz, 3.175 GHz to 3.476 GHz, 4.529 GHz to 4.761 GHz, and 5.254 to 5.513 GHz for IoT, LTE, and 5G new radio applications. CST simulator is used for simulating the antenna, and the fabricated prototype is also tested for measured values. Important parameters of MIMO like ECC and realized gain of MIMO prototype are measured to see the correlation between the antenna elements. The paper contains six sections. The proposed design is given in Section 2. Section 3 gives the measured values of MIMO prototype. Measured and simulated parameters of MIMO like ECC and realized gain are shown in Section 4. The state-of-art comparison and conclusion are given in Section 5 and Section 6 respectively.

2. PROPOSED MIMO ANTENNA

A 65 mm × 90 mm × 1.6 mm FR-4 substrate ($\tan\delta = 0.02$ and $\varepsilon r = 4.4$) is used for fabricating the proposed MIMO antenna as shown in Fig. 1. Four antennas (antenna 1–antenna 4) are placed at four corners on the top of the substrate. A slotted ground is present at the bottom of the substrate which is connected to the top four antenna elements. Antennas 1, 2, 3, and 4 cover multiple wireless bands which use sub-1 GHz, IoT/RFID, and sub-6 GHz platforms. Dimensions of MIMO system are listed in Table 1.

2.1. Working Mechanism of the Proposed MIMO

2.1.1. Single Element

Initially, the ground is designed using the equivalent area method [3]. The edges of the ground are then tapered as shown in Fig. 1(b) to free up more space and thus accommodate multiple antennas for efficient MIMO implementation. Antenna size is an important parameter in latest wireless applications. Since size and frequency are inversely related to each other, the antenna size needs to be increased to cover lower frequency bands, but this is not feasible due to size limitations. So, for sub-1 GHz band like LTE 700 MHz, a slotted ground given in Fig. 1(b) is used. When slots are added, there is an increase in the surface current area which reduces the frequency. As discussed in Section 2, four planar multiband antennas in MIMO configuration are placed at four corners on top of the substrate. The individual antenna element is a modified meandered antenna. Initially, a meandered antenna having length $\lambda/4$ is designed to cover frequencies below 1 GHz. Here λ denotes the patch wavelength at 700 MHz (the lowest

Table 1. Dimensions of MIMO system.

Param.	Size (mm)	Param.	Size (mm)	Param.	Size (mm)
$a1$	65	$p1$	3	c	20.2
$b1$	90	$q1$	1	d	14.2
$c1$	36.6	$r1$	7.5	e	66
$d1$	10	$s1$	5	f	8
$e1$	5.6	$t1$	3	g	19
$f1$	14	$u1$	6	h	10
$g1$	4	$v1$	8	i	2
$h1$	26	$w1$	24.5	j	8
$i1$	11	$x1$	3	k	14
$j1$	18	$y1$	19	m	4
$k1$	2	$z1$	2.5	n	22
$m1$	5	a	65		
$n1$	27	b	90		

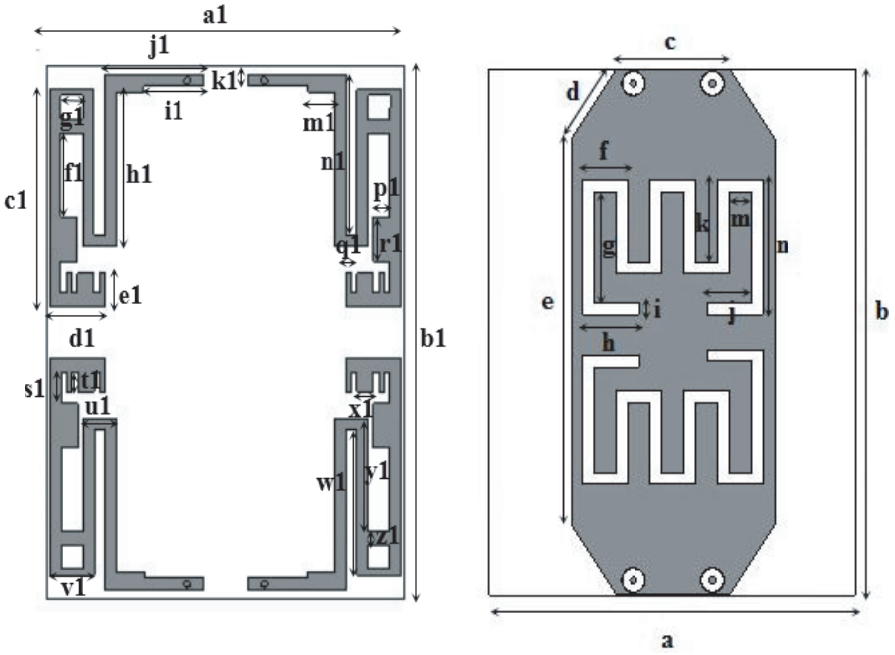

Figure 1. MIMO topology. (a) Top view. (b) Bottom view.

desired frequency). The matching of this antenna was not good, so for better impedance matching, the antenna was then modified and optimized by adding stubs to the meandered antenna. Due to the generation of higher order modes, the proposed antenna also covers important bands like 1.9 GHz to 2.1 GHz, 3.175 GHz to 3.476 GHz, 4.529 GHz to 4.761 GHz, and 5.254 to 5.513 GHz for IoT, RFID, and 5G new radio applications.

In order to achieve good isolation, two meandered slots were introduced in the partial ground plane. They minimized the current localization due to common ground, thereby increasing the port isolation. The slots also increased the surface current area which contributed to lowering the below

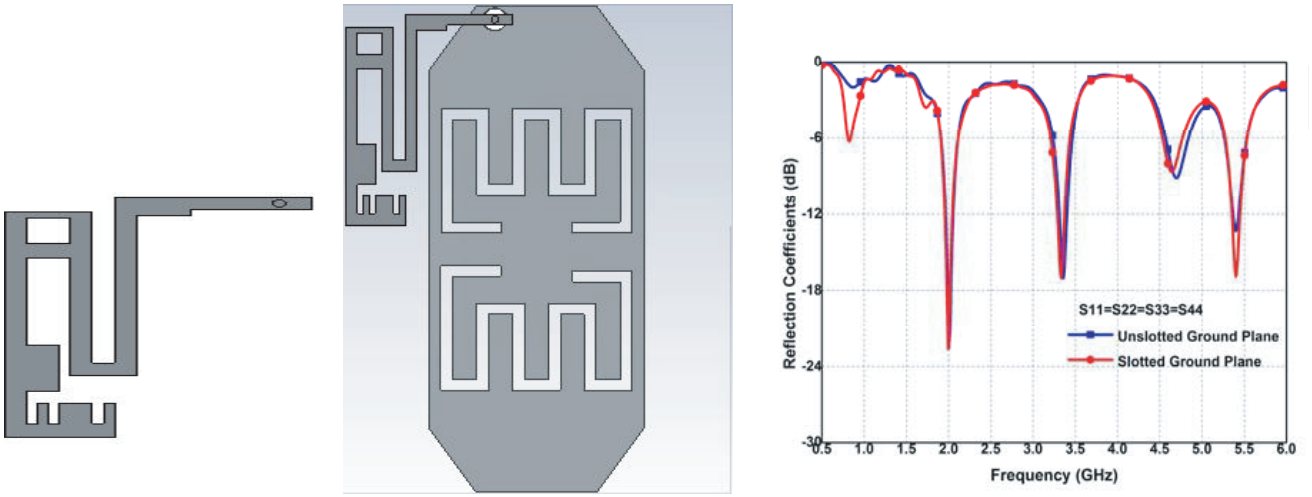

(a) (b) (c)

Figure 2. (a) Antenna element, (b) ground plane integration and (c) S-parameters of single element (with unslotted and slotted ground).

1 GHz frequencies, thereby further increasing the −6 dB impedance matching bandwidth. The antenna topology, its integration with ground, and the simulated S-parameters for slotted and unslotted grounds are presented in Fig. 2(a), Fig. 2(b), and Fig. 2(c), respectively. The return loss is below the standard value of −6 dB in the desired bands.

2.1.2. 4-Port MIMO Implementation and Coupling Mechanism

MIMO implementation is very important for improving the channel capacity, range, and reliability in a communication systems. When the four MIMO antenna elements are connected to the same ground as shown in Fig. 1, there is a change in the values of S-parameters due to mutual coupling between them. The separation between the ports is one of the major factors which affects the isolation in the MIMO antennas. Since isolation improvement becomes more challenging for the lower frequencies, S_{12} and S_{34} are usually low below 1 GHz band due to size constraint for portable devices. ECC depends on how strongly the radiated fields from MIMO elements interact with each other. When this interaction is strong, ECC increases which in turn reduces the performance of MIMO. So, in order to have ECC < 0.5, the MIMO antennas in the proposed design are placed in such a way that the beam directions of ports are different, and the overlapping between them is less. Also, to reduce current localization, slots were added in ground. Fig. 3(a) shows that antennas 1, 2, 3, and 4 cover the bands like 674 MHz to 1 GHz, 1.9 GHz to 2.1 GHz, 3.175 GHz to 3.476 GHz, 4.529 GHz to 4.761 GHz, and 5.254 to 5.513 GHz for IoT, RFID, and 5G new radio applications. The isolation parameters are shown in Fig. 3(b). The plot shows good isolation (S_{12}, S_{21}, S_{34}, and S_{43}) between MIMO antennas, making the proposed design suitable for multiple next generation applications. ECC between MIMO elements 1 and 2 and between 3 and 4 is shown in Fig. 3(c) which is within the acceptable range (below 0.5).

2.1.3. Surface Current Analysis

Surface current analysis is important for understanding the working of MIMO system. It shows the location where most of the current is distributed which helps in understanding the coupling between antenna elements. The surface current density (J_s) on the proposed MIMO design is plotted in Fig. 4. The plots are obtained at frequencies 0.8 GHz and 5.2 GHz. Surface current density at a particular frequency is obtained by exciting one of the ports and match terminating the others to 50 ohm. It shows that maximum current is concentrated on the main port whereas a small portion of it is distributed on the overlapping parts, ground plane, and other ports. This is due to current localization which takes

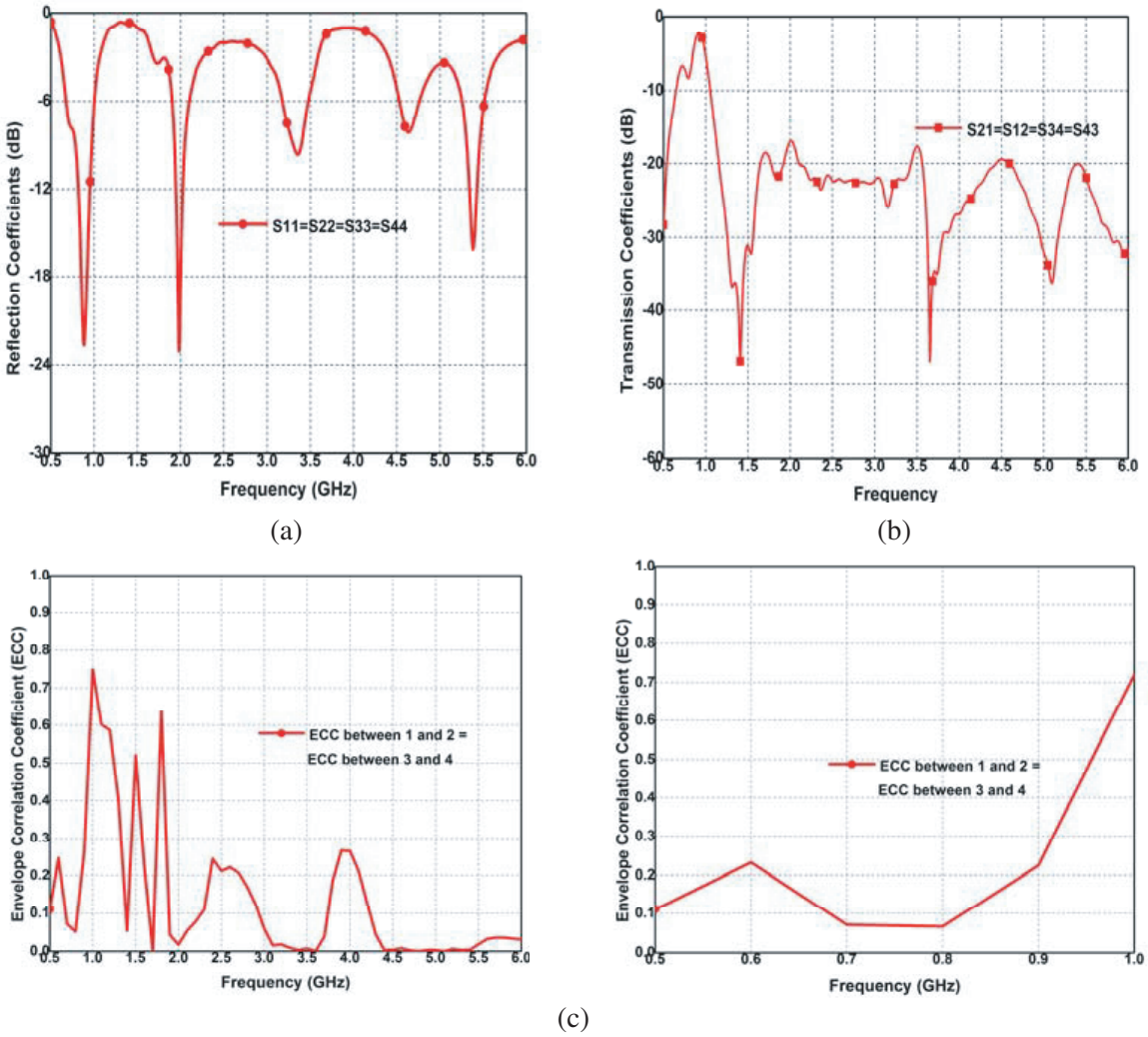

Figure 3. (a) S_{11}, S_{22}, S_{33} and S_{44}, (b) S_{12}, S_{21}, S_{34} and S_{43} and (c) ECC.

place when multiple antennas are integrated on the same common ground. The addition of slots localizes J_s on main antenna and thus improves the impedance matching. Isolation can be further improved by designing efficient decoupling networks while maintaining the compact size.

3. ANTENNA PROTOTYPE AND MEASUREMENTS

3.1. MIMO Prototype

The proposed prototype presented in Fig. 5 was fabricated in the Laboratory of Antenna Design, SMVD University, Jammu. Radiation pattern was measured in an anechoic chamber, and Anritsu vector network analyzer (MS2038C) was used for S-parameters measurement. Short, Open load and Through technique was used to calibrate the vector network analyser (VNA). For 5 kHz to 18 GHz band, the measurement setup had a dynamic range of 85 to 100 dB with a -60 dB noise floor. The intermediate frequency bandwidth of 10 kHz was used for the VNA. The VNA ports were connected to the antenna and SMA adapter using an N-type coaxial cable which was compensated by S_{21} calibration (available in VNA) of the chamber.

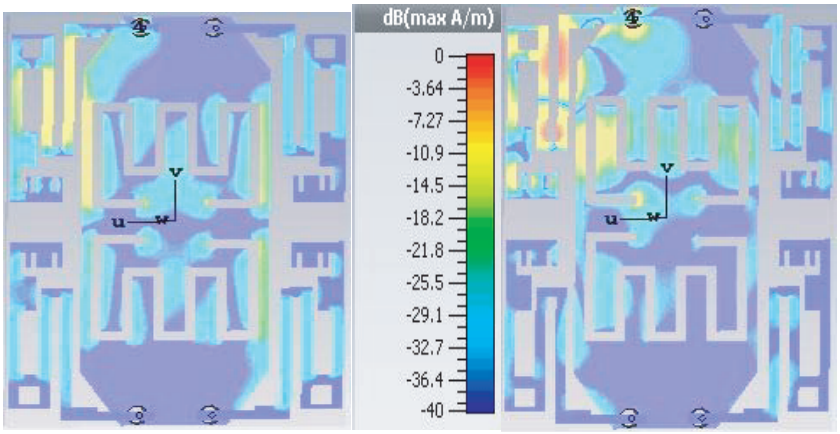

(a) (b)

Figure 4. Surface Current density (J_s) at (a) 0.8 GHz and (b) 5.2 GHz.

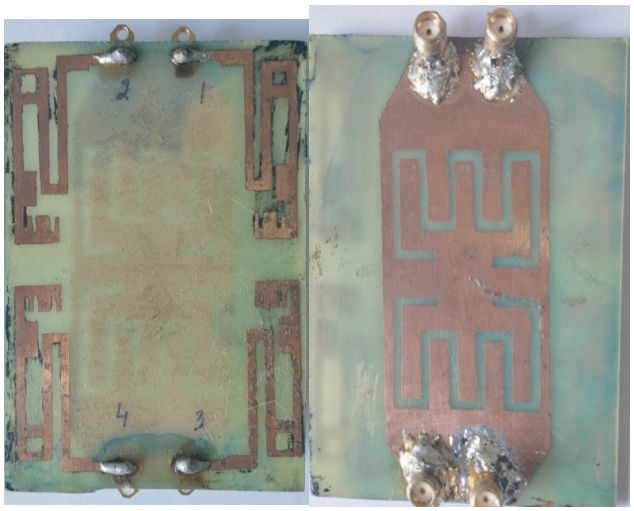

(a) (b)

Figure 5. Designed prototype, (a) front side and (b) backside.

3.2. Measured S-Parameters

S-parameters of port 1 (S_{11}), port 2 (S_{22}), port 3 (S_{33}), and port 4 (S_{44}) are presented in Fig. 6(a). It is seen that the antenna operates over a number of important frequency bands for modern applications like 674 MHz to 1 GHz (Bandwidth: 326 MHz), 1.9 GHz to 2.1 GHz (Bandwidth: 200 MHz), 3.175 GHz to 3.476 GHz (Bandwidth: 301 MHz), 4.529 GHz to 4.761 GHz (Bandwidth: 232 MHz), and 5.254 to 5.513 GHz (Bandwidth: 259 MHz). The measured isolation parameters as shown in Fig. 6(b) are in close agreement with the simulated values. Fabrication process slightly changes the port impedances which causes small differences between measured and simulated values.

3.3. Radiation Pattern

3.3.1. MIMO Realized Gain

Realized gain of MIMO is obtained from 3-D radiation pattern measured inside an anechoic chamber. The realized gains of port 1 to port 4 at 800 MHz and 5.2 GHz are presented in Table 2.

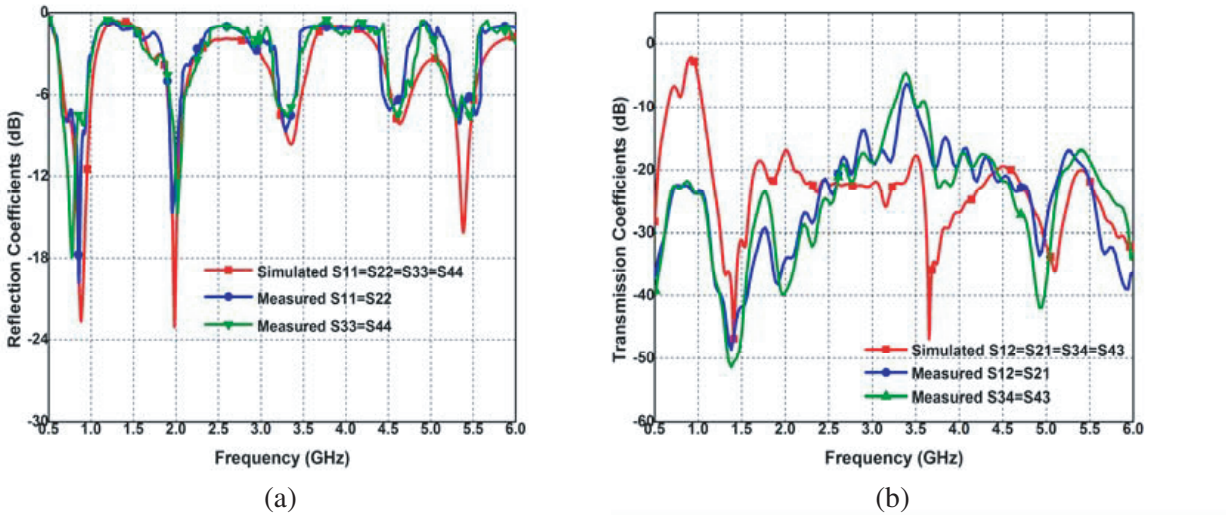

(a) (b)

Figure 6. (a) Reflection coefficients. (b) Transmission coefficients.

Table 2. MIMO realized gain.

MIMO Realized Gain (dBi)								
Results	**Port 1**		**Port 2**		**Port3**		**Port4**	
	800 MHz	**5.2 GHz**	**800 MHz**	**5.2 GHz**	**800 MHz**	**5.2 GHz**	**800 MHz**	**5.2 GHz**
Simulated	−6.46	1.06	−6.46	1.06	−6.46	1.06	−6.46	1.06
Measured	−4.31	−2.21	−4.16	−3.03	−4.24	−2.37	−3.97	−2.15

3.3.2. Radiation Efficiency

The maximum radiation efficiency of antenna is 78.37% at 3.2 GHz. The values of radiation efficiency at other frequencies in the desired bands of interest are given in Table 3.

Table 3. Radiation efficiency.

Frequency (GHz)	**Radiation efficiency (%)**	**Frequency (GHz)**	**Radiation efficiency (%)**	**Frequency (GHz)**	**Radiation efficiency (%)**
0.7	72.4	2.1	76.57	4.6	77.91
0.8	40.26	3.1	77.26	4.7	77.33
0.9	56.96	3.2	78.37	5.2	63.19
1.0	33.58	3.3	73.28	5.3	59.23
1.9	60	3.4	67.4	5.4	57.2
2.0	73.84	4.5	77.3	5.5	58.5

3.3.3. 2-D Radiation Pattern and Directivity

Normalized antenna radiation patterns (2-D) for MIMO antenna elements are given in Figs. 7 to 10. Figs. 7(a) and 7(b) present the 2-D pattern of port 1 at 800 MHz and 5.2 GHz, respectively. Figs. 8(a)

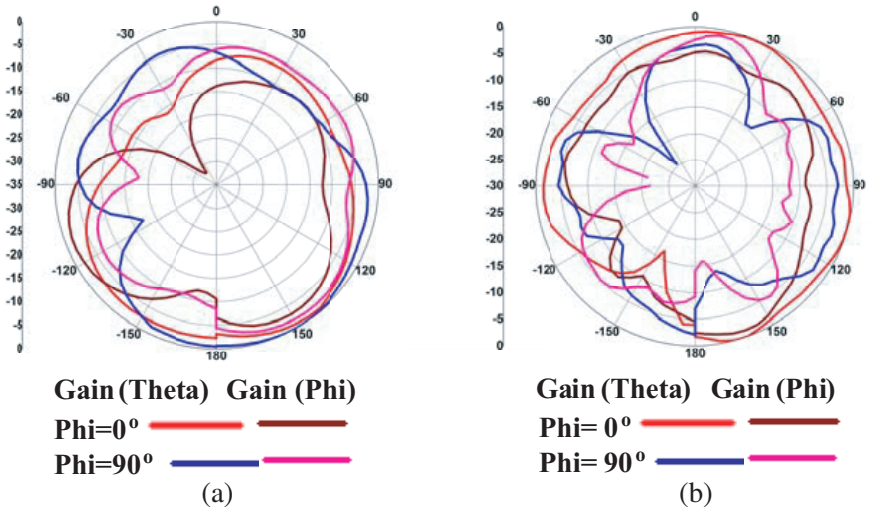

Figure 7. Measured 2-D pattern (port 1) at (a) 800 MHz and (b) 5.2 GHz.

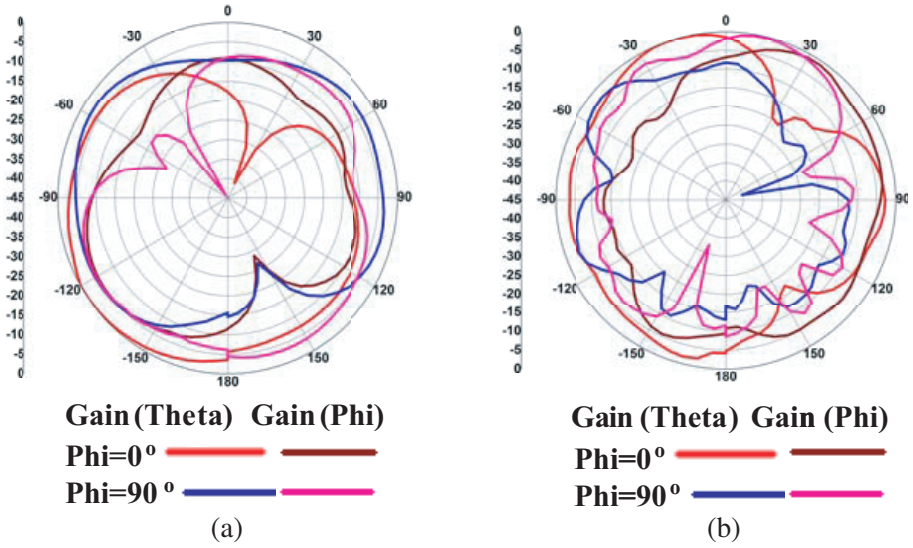

Figure 8. Measured 2-D pattern (port 2) at (a) 800 MHz and (b) 5.2 GHz.

and 8(b) present the 2-D pattern of port 2 at 800 MHz and 5.2 GHz, respectively. The 2-D pattern of port 3 at 800 MHz and 5.2 GHz is shown in Figs. 9(a) and 9(b), respectively, and for port 4 at 800 MHz and 5.2 GHz, it is presented in Figs. 10(a) and 10(b), respectively. The values of directivity calculated from radiation pattern measurements are given in Table 4.

Table 4. Antenna directivity calculated from measurements.

Directivity (dBi)								
Results	**Port 1**		**Port 2**		**Port3**		**Port4**	
	800 MHz	**5.2 GHz**	**800 MHz**	**5.2 GHz**	**800 MHz**	**5.2 GHz**	**800 MHz**	**5.2 GHz**
Simulated	2.29	5.26	2.29	5.26	2.29	5.26	2.29	5.26
Measured	1.78	5.22	1.92	5.16	2.03	5.17	1.73	5.13

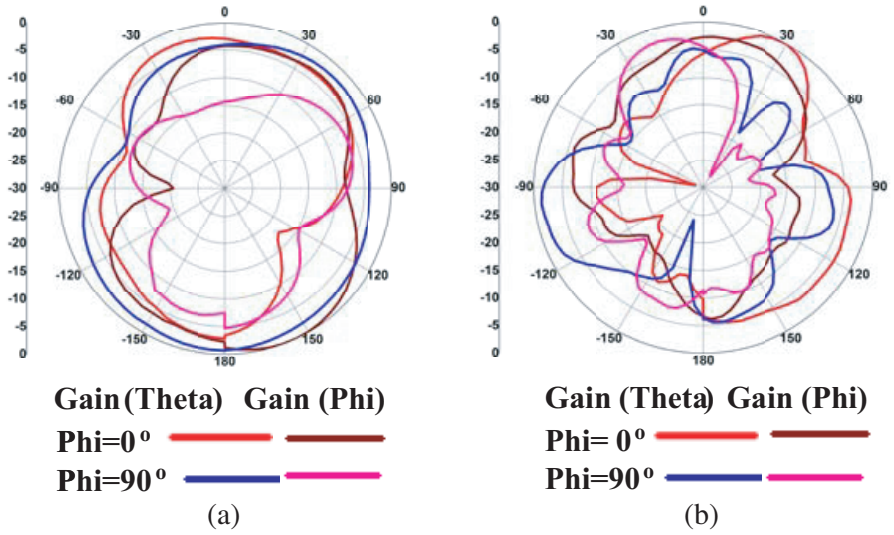

Figure 9. Measured 2-D pattern (port 3) at (a) 800 MHz and (b) 5.2 GHz.

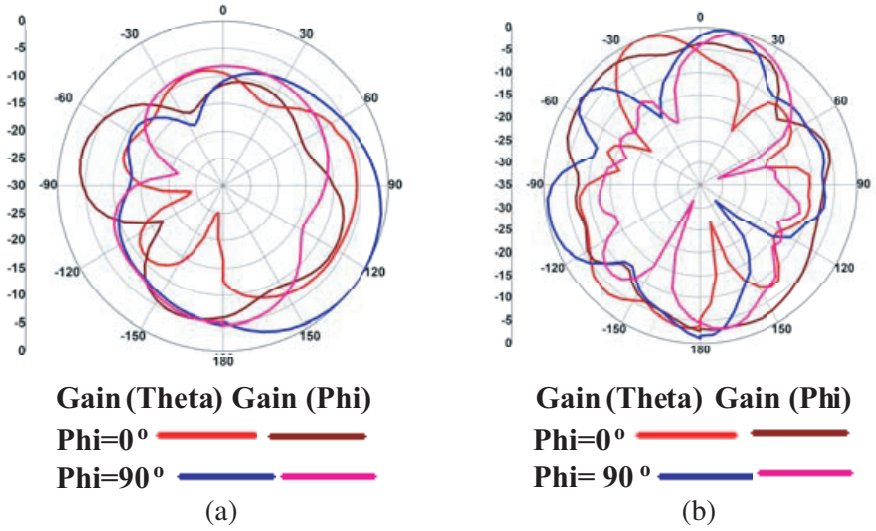

Figure 10. Measured 2-D pattern (port 4) at (a) 800 MHz and (b) 5.2 GHz.

4. MIMO ENVELOPE CORRELATION COEFFICIENT (ECC)

ECC is calculated between ports 1 and 2 and ports 3 and 4 from measured radiation pattern using the following equation:

$$Envelope\ Correlation\ Coefficient = \frac{\left|\iint_{4\pi} \overrightarrow{F_i}(\theta,\phi)\cdot\overrightarrow{F_j}(\theta,\phi)^*\,\partial\Omega\right|^2}{\iint_{4\pi}\left|\overrightarrow{F_i}(\theta,\phi)\right|^2\partial\Omega\iint_{4\pi}\left|\overrightarrow{F_j}(\theta,\phi)\right|^2\partial\Omega} \tag{1}$$

where $\overrightarrow{F_i}(\theta,\phi)$ and $\overrightarrow{F_j}(\theta,\phi)$ denote the radiation patterns for elements i and j, respectively, and $\cdot$ is the Hermitian multiplication [37]. For MIMO implementation of antenna elements, the value of ECC should be below 0.5 [37]. Table 5 shows the values of envelope correlation coefficients (simulated and measured) between antennas 1 and 2 at 800 MHz and between 3 and 4 at 800 MHz. The values are below

Table 5. ECC.

Port 1&2			Port 3&4		
Frequency (MHz)	Simulated	Measured	Frequency (MHz)	Simulated	Measured
800	0.0519	0.072	800	0.0519	0.0647

0.5 making it desirable for MIMO configuration. Due to experimental limitations, small differences are found between measured and simulated values.

5. STATE-OF-ART-COMPARISON

Comparison of some recent works with the proposed work is presented in Table 6. It shows that the proposed design is a compact multiband antenna that can be widely used in next generation applications like sub-1 GHz, IoT/RFID, and sub-6 GHz 5G new radio.

Table 6. Comparative analysis.

Reference	Size (mm^3)	Frequencies Covered (GHz)	Configuration	Max Realized Gain (dBi)	Max Efficiency (%)	Minimum Isolation (dB)
[26]	$68 \times 51 \times 1.6$	2.6 to 3.7	SISO	Not available	Not available	Not available
[27]	$11.5 \times 8.4 \times 1.6$	2.39 to 2.62, 2.69 to 3.0	SISO	2.01 (at 2.39 GHz)	54.9 (at 2.39 GHz)	–
[29]	$40 \times 36 \times 1.66$	5 to6	SISO	1.87 (at 5 GHz)	Not available	16
[30]	$21 \times 9 \times 0.8$	3.2 to 4.5, 4.3 to 7.8, 7.9 to 11.2	SISO	Not available	Not available	Not available
[31]	$80 \times 65 \times 1.5$	2.6 to 2.7	SISO	5.78 (at 4.5 GHz)	Not available	18
[33]	$63 \times 63 \times 1.52$	5.7 to 5.4	SISO	Not available	75.0 (at 5.0 GHz)	15
[38]	$45 \times 45 \times 0.8$	1.54 to 2.28, 2.28 to 2.85	SISO	Not available	Not available	Not available
[39]	$65 \times 120 \times 1.56$	0.78 to 1.2, 1.49 to 1.76, 0.61 to 0.92, 1.21 to 1.43, 0.94 to 1.35	MIMO	1.77 (at 1.04 GHz)	Not available	12.17
Proposed	$65 \times 90 \times 1.6$	674 to 1, 1.9 to 2.1, 3.175 to 3.476, 4.529 to 4.761 and 5.254 to 5.513	MIMO	3.215 (at 2 GHz)	78.37 (at 3.2 GHz)	20

6. CONCLUSION

A 4-port planar multiband MIMO antenna is proposed which covers a wide range of frequencies from 674 MHz to 1 GHz, 1.9 GHz to 2.1 GHz, 3.175 GHz to 3.476 GHz, 4.529 GHz to 4.761 GHz, and 5.254 to 5.513 GHz for Long term evolution (LTE), Internet of Things (IoT), and sub-6 GHz 5G new radio applications and thus can be used for latest applications like robotic navigation, logistics, healthcare, tracking, transportation, etc. Due to very small ECC between the ports (< 0.5), the MIMO configuration can be efficiently implemented which helps in increasing the data rates. It is very compact in size and thus can be used for portable handheld devices. Also, to determine the utility of the proposed antenna in various IoT applications, the antenna under test (AUT) can be configured to various communication modules like global system of mobile (GSM) and UHF RFID reader modules. It is also possible to integrate other platforms like wireless sensor networks (WSN) operating in these frequency bands by adopting a multiplexing technique. Since WSN and RFID are two constituents of the IoT platform, the antenna may find its application in IoT environment in addition to the internet connectivity and cellular services.

REFERENCES

1. Shereen, M. K., M. I. Khattak, and J. Nebhen, "A review of achieving frequency reconfiguration through switching in microstrip patch antennas for future 5G applications," *Alexandria Engineering Journal*, Vol. 61, No. 1, 29–40, 2022.
2. Kim, G. and K. Sangkil, "Design and analysis of dual polarized broadband microstrip patch antenna for 5G mmwave antenna module on FR4 substrate," *IEEE Access*, Vol. 9, 64306–64316, 2021.
3. Kumar, G. and K. P. Ray, *Broadband Microstrip Antennas*, Artech House, London, U.K., 2003.
4. Haykin, S., "Cognitive radio: Brain-empowered wireless communications," *IEEE Journal on Selected Areas in Communications*, Vol. 23, No. 2, 201–220, 2005.
5. Tawk, Y., J. Costantine, and C. Christodoulou, *Antenna Design for Cognitive Radio*, Artech House Boston, USA, 2016.
6. De Flaviis, F., L. Jofre, J. Romeu, and A. Grau, "Multiantenna systems for MIMO communications," *Synthesis Lectures on Antennas*, Vol. 3, No. 1, 1–250, 2008.
7. Varzakas, P., "Estimation of radio capacity of a spread spectrum cognitive radio rayleigh fading system," *ACM Proceedings of the 17th Pan-Hellenic Conference on Informatics with international participation*, 63–66, 2013.
8. Bakulin, M. G., V. B. Kreindelin, and D. Y. Pankratov, "Analysis of the capacity of MIMO channel in fading conditions," *2018 Systems of Signal Synchronization, Generating and Processing in Telecommunications (SYNCHROINFO)*, 1–6, 2018.
9. Chitra, M. P., S. Divya, M. Premkumar, V. Tamilselvi, and N. Karthika, "MIMO cognitive radio capacity in flat fading channel," *2017 Third International Conference on Science Technology Engineering & Management (ICONSTEM)*, 915–919, 2017.
10. Cheng, B. and Z. Du, "Dual polarization MIMO antenna for 5G mobile phone applications," *IEEE Transactions on Antennas and Propagation*, Vol. 69, No. 7, 4160–4165, 2020.
11. Chen Y. S. and C. P. Chang, "Design of a four-element multiple-input–multiple-output antenna for compact long-term evolution small-cell base stations," *IET Microwaves, Antennas & Propagation*, Vol. 10, No. 4, 385–392, 2016.
12. Chen, W. S. and K. H. Lai, "Compact design of MIMO antennas for LTE 700 application," *2015 IEEE International Symposium on Antennas and Propagation & USNC/URSI National Radio Science Meeting*, 1148–1149, 2015.
13. Singh, H. S., G. K. Pandey, P. K. Bharti, and M. K. Meshram, "Compact printed diversity antenna for LTE700/GSM1700/1800/UMTS/Wi-Fi/Bluetooth/LTE2300/2500 applications for slim mobile handsets," *Progress In Electromagnetics Research C*, Vol. 56, 83–91, 2015.

14. Krishnamoorthy, R., A. Desai, R. Patel, and A. Grover, "4 element compact triple band MIMO antenna for sub-6 GHz 5G wireless applications," *Wireless Networks*, Vol. 27, No. 6, 3747–3759, 2021.
15. Jaglan, N., S. D. Gupta, and M. S. Sharawi, "18 element massive MIMO/diversity 5G smartphones antenna design for sub-6 GHz LTE bands 42/43 applications," *IEEE Open Journal of Antennas and Propagation*, Vol. 2, 533–545, 2021.
16. Cha, J., C.-S. Leem, I. Kim, H. Lee, and H. Lee, "Broadband dual-polarized 2×2 MIMO antenna for a 5G wireless communication system," *Electronics*, Vol. 10, No. 17, 2141, 2021.
17. Hussain, R., "Shared-aperture slot-based sub-6-GHz and mm-wave IoT antenna for 5G applications," *IEEE Internet of Things Journal*, Vol. 8, No. 13, 10807–10814, 2021.
18. Wang, W., Z. Zhao, Z. Fang, Q. Sun, X. Liao, K. Y. See, and Y. Zheng, "Compact broadband four-port MIMO antenna for 5G and IoT applications," *2019 IEEE Asia-Pacific Microwave Conference (APMC)*, 1536–1538, 2019.
19. Li, S., X. L. Da, and S. Zhao, "The internet of things: A survey," *Information Systems Frontiers*, 243–259, 2015.
20. Zaman, M. R., R. Azim, N. Misran, M F. Asillam, and T. Islam, "Development of a semielliptical partial ground plane antenna for RFID and GSM-900," *International Journal of Antennas and Propagation*, 2014.
21. Bukhari, B., C. Singh, K. R. Jha, and S. K. Sharma, "Planar MIMO antennas for IoT and CR applications," *2017 IEEE Applied Electromagnetics Conference (AEMC)*, 1–2, 2017.
22. Bashir, U., K. R. Jha, G. Mishra, G. Singh, and S. K. Sharma, "Octahedron-shaped linearly polarized antenna for multistandard services including RFID and IoT," *IEEE Transactions on Antennas and Propagation*, Vol. 65, No. 7, 3364–3373, 2017.
23. Ebrahimi, E. and P. S. Hall, "A dual port wide-narrowband antenna for cognitive radio," *2009 3rd European Conference on Antennas and Propagation*, 809–812, 2009.
24. Al-Husseini, M., Y. Tawk, C. G. Christodoulou, K. Y. Kabalan, and A. El Hajj, "A reconfigurable cognitive radio antenna design," *2010 IEEE Antennas and Propagation Society International Symposium*, 1–4, 2010.
25. Tawk, Y., J. Costantine, K. Avery, and C. G. Christodoulou, "Implementation of a cognitive radio front-end using rotatable controlled reconfigurable antennas," *IEEE Transactions on Antennas and Propagation*, Vol. 59, No. 5, 1773–1778, 2011.
26. Mansoul, A., F. Ghanem, M. R. Hamid, and M. Trabelsi, "A selective frequency-reconfigurable antenna for cognitive radio applications," *IEEE Antennas and Wireless Propagation Letters*, Vol. 13, 515–518, 2014.
27. Cao, Y., S. W. Cheung, X. L. Sun, and T. I. Yuk, "Frequency-reconfigurable monopole antenna with wide tuning range for cognitive radio," *Microwave and Optical Technology Letters*, Vol. 56, No. 1, 145–152, 2014.
28. Zheng, S. H., X. Y. Liu, and M. M. Tentzeris, "A novel optically controlled reconfigurable antenna for cognitive radio systems," *2014 IEEE Antennas and Propagation Society International Symposium (APSURSI)*, 1246–1247, 2014.
29. Erfani, E., J. Nourinia, C. Ghobadi, M. Niroo-Jazi, and T. A. Denidni, "Design and implementation of an integrated UWB/reconfigurable-slot antenna for cognitive radio applications," *IEEE Antennas and Wireless Propagation Letters*, Vol. 11, 77–80, 2012.
30. Srivastava, G., A. Mohan, and A. Chakrabarty, "Compact reconfigurable UWB slot antenna for cognitive radio applications," *IEEE Antennas and Wireless Propagation Letters*, Vol. 16, 1139–1142, 2016.
31. Nachouane, H., A. Najid, A. Tribak, and F. Riouch, "Dual port antenna combining sensing and communication tasks for cognitive radio," *International Journal of Electronics and Telecommunications*, Vol. 62, No. 2, 121–127, 2016.
32. Hu, Z. H., P. S. Hall, and P. Gardner, "Reconfigurable dipole-chassis antennas for small terminal MIMO applications," *Electronics Letters*, Vol 47, No. 17, 953–955, 2011.

33. Chacko, B. P., G. Augustin, and T. A. Denidni, "Electronically reconfigurable uniplanar antenna with polarization diversity for cognitive radio applications," *IEEE Antennas and Wireless Propagation Letters*, Vol. 14, 213–216, 2015.
34. Cheng, S. P. and K. H. Lin, "A reconfigurable monopole MIMO antenna with wideband sensing capability for cognitive radio using varactor diodes," *2015 IEEE International Symposium on Antennas and Propagation & USNC/URSI National Radio Science Meeting*, 2233–2234, 2015.
35. Tawk, Y., F. Ayoub, C. G. Christodoulou, and J. Costantine, "A MIMO cognitive radio antenna system," *2013 IEEE Antennas and Propagation Society International Symposium (APSURSI)*, 572–573, 2013.
36. Hussain, R. and M. S. Sharawi, "Integrated reconfigurable multiple-input-multiple-output antenna system with an ultra-wideband sensing antenna for cognitive radio platforms," *IET Microwaves, Antennas & Propagation*, Vol. 9, No. 9, 940–947, 2015.
37. Jha, K. R. and S. K. Sharma, "Combination of frequency agile and quasi-elliptical planar monopole antennas in MIMO implementations for handheld devices," *IEEE Antennas Propagation Mag.*, Vol. 60, 118–131, 2018.
38. Fakharian, M. M., P. Rezaei, and A. A. Orouji, "A novel slot antenna with reconfigurable meander-slot DGS for cognitive radio applications," *Applied Computational Electromagnetics Society Journal (ACES)*, Vol. 30, No. 7, 748–753, 2015.
39. Hussain, R. and M. S. Sharawi, "Planar four-element frequency agile MIMO antenna system with chassis mode reconfigurability," *Microwave and Optical Technology Letters*, Vol. 57, No. 8, 1933–1938, 2015.